Int. J. Mech. Sci. Pergamon Press Ltd. 1967. Vol. 9, pp. 83–96. Printed in Great Britain

DYNAMICS OF THE BIFILAR PENDULUM

T. R. KANE and GAN-TAI TSENG*
Division of Engineering Mechanics, Stanford University, Stanford, California

(*Received* 9 *August* 1966)

Summary—The full nonlinear equations of motion of a bifilar pendulum are derived without the aid of simplifying assumptions about the geometry of the suspension or the inertia properties of the suspended body. Two examples of practical interest are discussed. The first involves cables of unequal length, and the second deals with effects of principal axes misalignment.

The nonlinear equations serve also as the point of departure for a rational attack on a problem of tilting oscillations. Torsional motions of the kind employed for moment of inertia measurements are represented by an exact solution of the nonlinear equations of motion, and a linearization about this solution then permits the formulation of stability criteria in terms of Floquet theory. The physical significance of instabilities thus discovered is studied by reference to specific examples.

NOTATION

b, b'	distances between points of attachment
l, l'	cable lengths
$\mathbf{n}_i, \tilde{\mathbf{n}}_i, \mathbf{b}_i$	unit vectors
θ_i	orientation angle
s_i, c_i	$\sin\theta_i, \cos\theta_i$
L, B	$l/b', b/b'$
$\beta_1, \ldots, \beta_5$	equations (4)
γ_i	β_i/β_5
n_{ij}	equations (8)
$b_{ij}, \tilde{b}_{ij}$	components of $\mathbf{b}_i$
$\boldsymbol{\omega}$	angular velocity
Ω_i, ω_i	components of $\boldsymbol{\omega}$
$\boldsymbol{\alpha}$	angular acceleration
A_i, α_i	components of $\boldsymbol{\alpha}$
$\mathbf{r}$	relative position vector of mass center
r	magnitude of $\mathbf{r}$
$\mathbf{v}$	velocity of mass center
λ	angle between $\mathbf{r}$ and $\tilde{\mathbf{n}}_3$
s_λ, c_λ	$\sin\lambda, \cos\lambda$
v_{ij}	equations (24)
$\mathbf{a}$	acceleration of mass center
a_i	component of $\mathbf{a}$
Ω_{ij}	equations (28)
$\boldsymbol{\omega}_{,\dot{\theta}_r}$	partial rate of change of orientation
$\mathbf{v}_{,\dot{\theta}_r}$	partial rate of change of position
m	mass
g	acceleration of gravity
F_r, F_r^*	generalized forces
$\mathbf{T}$	inertia torque
T_i	component of $\mathbf{T}$

* Airsearch Manufacturing Company, Los Angeles, California.

I_i	principal moment of inertia
$q_1, \ldots, q_5$	$\theta_1, \ldots, \theta_5$
$q_6, \ldots, q_{10}$	$\dot{\theta}_1, \ldots, \dot{\theta}_5$
N_i	equations (47)
f	equations (48)
t^*	period
q_i^*	periodic function
ε_i	perturbation
Z_{ij}	function of q_k^*
Z, H	matrices
λ_i	eigenvalue

INTRODUCTION

A BIFILAR pendulum consists of a rigid body suspended by two wires or cables. Frequently, such an arrangement is employed for the experimental determination of moments of inertia, the essence of the method being that measured values of the period of torsional vibrations are substituted into a formula derived from an analytical description of these oscillations. Usually, the derivation of the formula involves either complete or partial linearization of the equations of motion. This not only simplifies the analysis considerably, but is generally justified by the fact that it does not impair the accuracy of the results. However, certain modes of behavior of the system fall outside of the scope of such a theory. For example, in practice one sometimes encounters the potentially dangerous phenomenon of parasitic "tilting" oscillations with time-dependent, increasing amplitude, and one finds that the occurrence of such motions is intimately related to the geometry of the suspension, i.e. to the lengths of the cables, the distance between points of attachment, etc. These vibrations, it turns out, can be treated analytically only by taking into account nonlinearities that are normally ignored.

In the present paper, the full nonlinear equations of motion of the bifilar pendulum are derived without the aid of simplifying assumptions about the geometry of the suspension or the inertia properties of the suspended body. To illustrate the use of these equations, two examples of practical interest are discussed. The first involves cables of unequal length, and the second deals with effects of principal axes misalignment.

The nonlinear equations serve also as the point of departure for a rational attack on the previously mentioned problem of tilting oscillations. Torsional motions of the kind employed for moment of inertia measurements are here represented by an exact solution of the nonlinear equations of motion, and a linearization about this solution then permits the formulation of stability criteria in terms of Floquet theory. The physical significance of instabilities thus discovered is studied by reference to specific examples.

EQUATIONS OF MOTION

The geometric quantities that are to be used to describe the motion of a bifilar pendulum are shown in Fig. 1, where A and B designate the points at which cables are attached to a horizontal support, C and D are the points at which the cables are fastened to a rigid body R, and R^* is the mass center of this body. The angle θ_1 measures rotations of R about line CD, and $\theta_2, \ldots, \theta_5$ serve to determine the orientations of lines BC and CD.

The latter angles are not independent of each other, because the orientations of BC and CD must be such that the sum of the vectors $\vec{AB}$, $\vec{BC}$ and $\vec{CD}$ is equal to $\vec{AD}$. If $\mathbf{n}_1$,

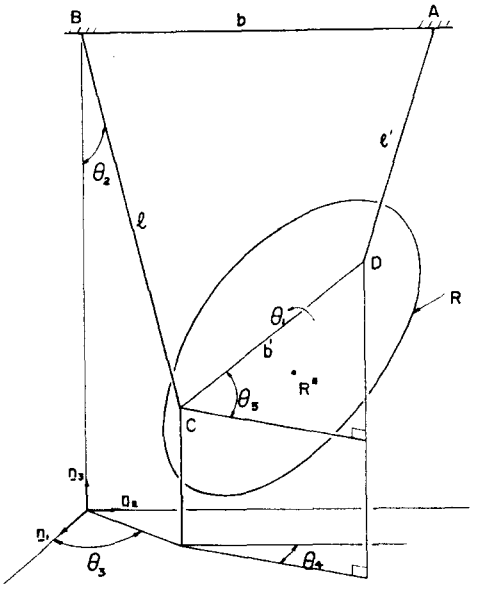

FIG. 1. Bifilar pendulum.

$\mathbf{n}_2$ and $\mathbf{n}_3$ comprise a right-handed set of mutually perpendicular unit vectors directed as shown, this condition can be expressed as

$$-b\mathbf{n}_2+l[s_2(c_3\,\mathbf{n}_1+s_3\,\mathbf{n}_2)-c_2\,\mathbf{n}_3]+b'[c_5(s_4\,\mathbf{n}_1+c_4\,\mathbf{n}_2)+s_5\,\mathbf{n}_3]=\vec{AD} \tag{1}$$

where s_i and c_i denote $\sin\theta_i$ and $\cos\theta_i$, respectively; and scalar multiplication of each side of equation (1) with itself leads to the constraint equation

$$(ls_2\,c_3+b's_4\,c_5)^2+(-b+ls_2\,s_3+l'c_4\,c_5)^2+(-lc_2+b's_5)^2=(l')^2 \tag{2}$$

One way to take this equation into account is to regard the five quantities $\theta_1,\ldots,\theta_5$ as generalized co-ordinates of a simple nonholonomic system possessing only four degrees of freedom, and to convert equation (2) into a differential constrain equation by differentiating it with respect to time. This gives

$$\beta_1\dot{\theta}_1+\beta_2\dot{\theta}_2+\beta_3\dot{\theta}_3+\beta_4\dot{\theta}_4-\beta_5\dot{\theta}_5=0 \tag{3}$$

where

$$\left.\begin{aligned}
\beta_1 &= 0\\
\beta_2 &= L[c_2\,c_3(Ls_2\,c_3+s_4\,c_5)+c_2\,s_3(-B+Ls_2\,s_3+c_4\,c_5)+s_2(-Lc_2+s_5)]\\
\beta_3 &= L[-s_2\,s_3(Ls_2\,c_3+s_4\,c_5)+s_2\,c_3(-B+Ls_2\,s_3+c_4\,c_5)]\\
\beta_4 &= c_4\,c_5(Ls_2\,c_3+s_4\,c_5)-s_4\,c_5(-B+Ls_2\,s_3+c_4\,c_5)\\
\beta_5 &= s_4\,s_5(Ls_2\,c_3+s_4\,c_5)+c_4\,s_5(-B+Ls_2\,s_3+c_4\,c_5)-c_5(-Lc_2+s_5)
\end{aligned}\right\} \tag{4}$$

with L and B defined as

$$L=l/b',\quad B=b/b'$$

In the sequel, it becomes necessary to solve equation (3) for $\dot{\theta}_5$. For computational reasons, it is convenient to express the result as

$$\dot{\theta}_5=\sum_{i=1}^{4}\gamma_i\dot{\theta}_i \tag{5}$$

where $\gamma_1, \ldots, \gamma_4$ are known functions of $\theta_1, \ldots, \theta_5$, namely

$$\gamma_i = \beta_i/\beta_5, \quad i = 1, \ldots, 4 \tag{6}$$

We turn now to the derivation of expressions for the angular velocity and angular acceleration of the body R and for the velocity and acceleration of the mass center R* of R. As some of these quantities shall have to be referred to body-fixed axes, we introduce two further right-handed sets of base vectors: $\tilde{\mathbf{n}}_1, \tilde{\mathbf{n}}_2, \tilde{\mathbf{n}}_3$, directed as shown in Fig. 2; and

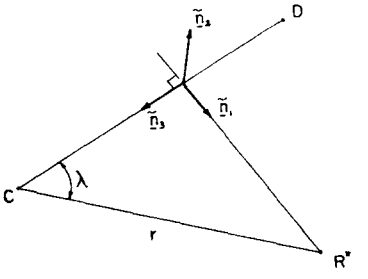

FIG. 2. Unit vectors.

$\mathbf{b}_1, \mathbf{b}_2, \mathbf{b}_3$, respectively parallel to principal axes of inertia of R for R*. The relationship between the first of these sets and $\mathbf{n}_1, \mathbf{n}_2, \mathbf{n}_3$ depends on θ_1, θ_4 and θ_5, and is given by

$$\tilde{\mathbf{n}}_i = \sum_{j=1}^{3} n_{ij}\,\mathbf{n}_j, \quad i = 1, 2, 3 \tag{7}$$

where

$$\left.\begin{array}{lll} n_{11} = s_1 c_4 + c_1 s_4 s_5 & n_{12} = -s_1 s_4 + c_1 c_4 s_5 & n_{13} = -c_1 c_5 \\ n_{21} = c_1 c_4 - s_1 s_4 s_5 & n_{22} = -c_1 s_4 - s_1 c_4 s_5 & n_{23} = s_1 c_5 \\ n_{31} = -s_4 c_5 & n_{32} = -c_4 c_5 & n_{33} = -s_5 \end{array}\right\} \tag{8}$$

Next, the vectors $\mathbf{b}_1, \mathbf{b}_2, \mathbf{b}_3$ are related to $\tilde{\mathbf{n}}_1, \tilde{\mathbf{n}}_2, \tilde{\mathbf{n}}_3$ by

$$\mathbf{b}_i = \sum_{j=1}^{3} \tilde{b}_{ij}\,\tilde{\mathbf{n}}_j, \quad i = 1, 2, 3 \tag{9}$$

where $\tilde{b}_{ij}$ is a constant that depends only on the choice of the points of attachment C and D. Finally then, $\mathbf{b}_1, \mathbf{b}_2, \mathbf{b}_3$ are given in terms of $\mathbf{n}_1, \mathbf{n}_2, \mathbf{n}_3$ by

$$\mathbf{b}_i = \sum_{j=1}^{3} b_{ij}\,\mathbf{n}_j, \quad i = 1, 2, 3 \tag{10}$$

where

$$b_{ij} = \sum_{k=1}^{3} \tilde{b}_{ik}\, n_{kj} \tag{11}$$

The angular velocity $\boldsymbol{\omega}$ of R is expressed most directly as (see Figs. 1 and 2)

$$\boldsymbol{\omega} = \dot{\theta}_1 \tilde{\mathbf{n}}_3 - \dot{\theta}_4 \mathbf{n}_3 + \dot{\theta}_5 (c_4 \mathbf{n}_1 - s_4 \mathbf{n}_2) \tag{12}$$

and substitution from equations (7) and (8) leads to

$$\boldsymbol{\omega} = \sum_{i=1}^{3} \Omega_i\,\mathbf{n}_i \tag{13}$$

where

$$\left.\begin{array}{l} \Omega_1 = -s_4 c_5 \dot{\theta}_1 + c_4 \dot{\theta}_5 \\ \Omega_2 = -c_4 c_5 \dot{\theta}_1 - s_4 \dot{\theta}_5 \\ \Omega_3 = -s_5 \dot{\theta}_1 - \dot{\theta}_4 \end{array}\right\} \tag{14}$$

Alternatively, $\boldsymbol{\omega}$ can be referred to the body-fixed unit vectors $\mathbf{b}_1, \mathbf{b}_2, \mathbf{b}_3$ by setting

$$\boldsymbol{\omega} = \sum_{i=1}^{3} \omega_i\,\mathbf{b}_i \tag{15}$$

so that $\omega_i = \boldsymbol{\omega}.\mathbf{b}_i$. From equations (13) and (10) it then follows that

$$\omega_i = \sum_{j=1}^{3} b_{ij}\,\Omega_j, \quad i = 1, 2, 3 \tag{16}$$

Similarly, the angular acceleration $\boldsymbol{\alpha}$ of R can be expressed either as

$$\boldsymbol{\alpha} = \sum_{i=1}^{3} A_i\,\mathbf{n}_i \tag{17}$$

or as

$$\boldsymbol{\alpha} = \sum_{i=1}^{3} \alpha_i\,\mathbf{b}_i \tag{18}$$

where $A_i = \dot{\Omega}_i$ and $\alpha_i = \boldsymbol{\alpha}.\mathbf{b}_i$. Consequently

$$\left.\begin{aligned} A_1 &= -s_4 c_5 \ddot{\theta}_1 + c_4 \ddot{\theta}_5 - c_4 c_5 \dot{\theta}_1 \dot{\theta}_4 + s_4 s_5 \dot{\theta}_1 \dot{\theta}_5 - s_4 \dot{\theta}_4 \dot{\theta}_5 \\ A_2 &= -c_4 c_5 \ddot{\theta}_1 - s_4 \ddot{\theta}_5 + s_4 c_5 \dot{\theta}_1 \dot{\theta}_4 + c_4 c_5 \dot{\theta}_1 \dot{\theta}_5 - c_4 \dot{\theta}_4 \dot{\theta}_5 \\ A_3 &= -s_5 \ddot{\theta}_1 - \ddot{\theta}_4 - c_5 \dot{\theta}_1 \dot{\theta}_5 \end{aligned}\right\} \tag{19}$$

and equations (17) and (10) lead to

$$\alpha_i = \sum_{j=1}^{3} b_{ij}\,A_j \tag{20}$$

To find the velocity $\mathbf{v}$ of the point R*, we first express the position vector $\mathbf{r}$ of R* relative to point C in terms of the length r and the angle λ shown in Fig. 2, obtaining

$$\mathbf{r} = r(s_\lambda\,\tilde{\mathbf{n}}_1 - c_\lambda\,\tilde{\mathbf{n}}_3)$$

or, after using equations (7),

$$\mathbf{r} = \sum_{i=1}^{3} r_i\,\mathbf{n}_i \tag{21}$$

where

$$r_i = r(s_\lambda\,n_{1i} - c_\lambda\,n_{3i}), \quad i = 1, 2, 3 \tag{22}$$

The velocity $\mathbf{v}$ is then given by

$$\mathbf{v} = \mathbf{v}^C + \boldsymbol{\omega} \times \mathbf{r}$$

where $\mathbf{v}^C$ denotes the velocity of point C; and substitutions from equations (13), (14), (21) and (22) permit one to write the result as

$$\mathbf{v} = \sum_{i=1}^{3} \sum_{j=1}^{5} v_{ij}\,\dot{\theta}_j\,\mathbf{n}_i \tag{23}$$

where

$$\left.\begin{aligned} v_{11} &= r s_\lambda (c_1 c_4 - s_1 s_4 s_5) \\ v_{12} &= l c_2 c_3 \\ v_{13} &= -l s_2 s_3 \\ v_{14} &= r[s_\lambda(-s_1 s_4 + c_1 c_4 s_5) + c_\lambda c_4 c_5] \\ v_{15} &= r(-c_\lambda s_4 s_5 + s_\lambda c_1 s_4 c_5) \\ v_{21} &= -r s_\lambda (c_1 s_4 + s_1 c_4 s_5) \\ v_{22} &= l c_2 s_3 \\ v_{23} &= l s_2 c_3 \\ v_{24} &= -r[s_\lambda s_4 c_5 + s_\lambda(s_1 c_4 + c_1 s_4 s_5)] \\ v_{25} &= r(s_\lambda c_1 c_4 c_5 - c_\lambda c_4 s_5) \\ v_{31} &= r s_\lambda s_1 c_5 \\ v_{32} &= l s_2 \\ v_{33} &= v_{34} = 0 \\ v_{35} &= r(c_\lambda c_5 + s_\lambda c_1 s_5) \end{aligned}\right\} \tag{24}$$

Finally, differentiation of equation (23) leads to the following expression for the acceleration **a** of R*:

$$\mathbf{a} = \sum_{i=1}^{3} a_i \mathbf{n}_i \tag{25}$$

where

$$a_i = \sum_{j=1}^{5} (v_{ij}\dot{\theta}_j + v_{ij}\ddot{\theta}_j) \tag{26}$$

$$\left.\begin{aligned}
v_{11} &= -rs_\lambda[(s_1 c_4 + c_1 s_4 s_5)\dot{\theta}_1 + (c_1 s_4 + s_1 c_4 c_4 s_5)\dot{\theta}_4 + s_1 s_4 c_5 \dot{\theta}_5] \\
v_{12} &= -l(s_2 c_3 \dot{\theta}_2 + c_2 + s_3 \dot{\theta}_3) \\
v_{13} &= -l(c_2 s_3 \dot{\theta}_2 + s_2 c_3 \dot{\theta}_3) \\
v_{14} &= r[-s_\lambda(c_1 s_4 + s_1 c_4 s_5)\dot{\theta}_1 - (s_\lambda s_1 c_4 + s_\lambda c_1 s_4 s_5 + c_\lambda s_4 c_5)\dot{\theta}_4 + (s_\lambda c_1 c_4 c_5 - c_\lambda c_4 s_5)\dot{\theta}_5] \\
v_{15} &= r[-s_\lambda s_1 s_4 c_5 \dot{\theta}_1 + (s_\lambda c_1 c_5 - c_\lambda s_5) c_4 \dot{\theta}_4 - (c_\lambda s_4 c_5 + s_\lambda c_1 s_4 s_5)\dot{\theta}_5] \\
v_{21} &= -rs_\lambda[(c_1 c_4 s_5 - s_1 s_4)\dot{\theta}_1 + (c_1 c_4 - s_1 s_4 s_5)\dot{\theta}_4 + s_1 c_4 c_5 \dot{\theta}_5] \\
v_{22} &= l(-s_2 s_3 \dot{\theta}_2 + c_2 c_3 \dot{\theta}_3) \\
v_{23} &= l(c_2 c_3 \dot{\theta}_2 - s_2 s_3 \dot{\theta}_3) \\
v_{24} &= -r[s_\lambda(c_1 c_4 - s_1 s_4 s_5)\dot{\theta}_1 + (c_\lambda c_4 c_5 - s_\lambda s_1 s_4 + s_\lambda c_1 c_4 s_5)\dot{\theta}_4 + (s_\lambda c_1 s_4 c_5 - c_\lambda s_4 s_5)\dot{\theta}_5] \\
v_{25} &= r[-s_\lambda s_1 c_4 c_5 \dot{\theta}_1 + (c_\lambda s_5 - s_\lambda c_1 c_5) s_4 \dot{\theta}_4 - (s_\lambda c_1 c_4 s_5 + c_\lambda c_4 c_5)\dot{\theta}_5] \\
v_{31} &= rs_\lambda(c_1 c_5 \dot{\theta}_1 - s_1 s_5 \dot{\theta}_5) \\
v_{32} &= lc_2 \dot{\theta}_2 \\
v_{33} &= v_{34} = 0 \\
v_{35} &= r[-s_\lambda s_1 s_5 \dot{\theta}_1 + (s_\lambda c_1 c_5 - c_\lambda s_5)\dot{\theta}_5]
\end{aligned}\right\} \tag{27}$$

The method[1] that will be used to derive equations of motion requires the formulation of four partial rates of change of orientation of the body R and four partial rates of change of position of the point R*. The first four, denoted by $\boldsymbol{\omega}_{,\dot{\theta}_k}$, $k = 1, \ldots, 4$, are the coefficients of $\dot{\theta}_1, \ldots, \dot{\theta}_4$, respectively, in any expression for the angular velocity $\boldsymbol{\omega}$, provided $\dot{\theta}_5$ has first been eliminated by means of equation (5). Now, it follows from equations (14) and (5) that Ω_j can be expressed as

$$\Omega_j = \sum_{k=1}^{4} \Omega_{jk}\dot{\theta}_k, \quad j = 1, 2, 3$$

where

$$\left.\begin{aligned}
&\Omega_{11} = -s_4 c_5 \quad \Omega_{12} = c_4 \gamma_2 \quad \Omega_{13} = c_4 \gamma_3 \quad \Omega_{14} = c_4 \gamma_4 \\
&\Omega_{21} = -c_4 c_5 \quad \Omega_{22} = -s_4 \gamma_2 \quad \Omega_{23} = -s_4 \gamma_3 \quad \Omega_{24} = -s_4 \gamma_4 \\
&\Omega_{31} = -s_5 \quad \Omega_{32} = 0 \quad \Omega_{33} = 0 \quad \Omega_{34} = -1
\end{aligned}\right\} \tag{28}$$

and substitution into equations (16) thus gives

$$\omega_i = \sum_{j=1}^{3} \sum_{k=1}^{4} b_{ij}\Omega_{jk}\dot{\theta}_k, \quad i = 1, 2, 3 \tag{29}$$

The coefficients of $\dot{\theta}_1, \ldots, \dot{\theta}_4$ in equation (15) can now be identified, and it appears that

$$\boldsymbol{\omega}_{,\dot{\theta}_r} = \sum_{i=1}^{3} \sum_{j=1}^{3} b_{ij}\Omega_{jr}\mathbf{b}_i, \quad r = 1, \ldots, 4 \tag{30}$$

Similarly, the partial rates of change of position $\mathbf{v}_{,\dot{\theta}_r}$, $r = 1, \ldots, 4$, are the coefficients of $\dot{\theta}_1, \ldots, \dot{\theta}_4$, respectively, in equation (23) [after elimination of $\dot{\theta}_5$ by means of equation (5)]. Consequently

$$\mathbf{v}_{,\dot{\theta}_r} = \sum_{i=1}^{3} (v_{ir} + v_{i5}\gamma_r)\mathbf{n}_i, \quad r = 1, \ldots, 4 \tag{31}$$

Generalized active forces $F_1, \ldots, F_4$ are formed by scalar multiplications of the partial rates of change of position of R* with the weight force $-mg\mathbf{n}_3$, where m denotes the mass of the body R and g is the acceleration of gravity, i.e.

$$F_r = \mathbf{v}_{,\dot{\theta}_r} \cdot (-mg\mathbf{n}_3), \quad r = 1, \ldots, 4$$

or, in view of equations (31),

$$F_r = -mg(v_{3r} + v_{35}\gamma_r), \quad r = 1, \ldots, 4 \tag{32}$$

Similarly, generalized inertia forces $F_1^*, \ldots, F_4^*$ are given by

$$F_r^* = \mathbf{v}_{,\dot{\theta}_r} \cdot (-m\mathbf{a}) + \boldsymbol{\omega}_{,\dot{\theta}_r} \cdot \mathbf{T}, \quad r = 1, \ldots, 4 \tag{33}$$

where $\mathbf{T}$ is the so-called inertia torque. If I_1, I_2 and I_3 denote the principal moments of inertia of R for R*, then $\mathbf{T}$, resolved into components parallel to the unit vectors $\mathbf{b}_1$, $\mathbf{b}_2$, $\mathbf{b}_3$, is given by

$$\mathbf{T} = \sum_{i=1}^{3} T_i \mathbf{b}_i \tag{34}$$

where

$$\left.\begin{aligned} T_1 &= \omega_2 \omega_3 (I_2 - I_3) - \alpha_1 I_1 \\ T_2 &= \omega_3 \omega_1 (I_3 - I_1) - \alpha_2 I_2 \\ T_3 &= \omega_1 \omega_2 (I_1 - I_2) - \alpha_3 I_3 \end{aligned}\right\} \tag{35}$$

Substitution from equations (25), (30), (31) and (34) thus leads to

$$F_r^* = \sum_{i=1}^{3} \left[-ma_i(v_{ir} + v_{i5}\gamma_r) + \sum_{j=1}^{3} b_{ij}\Omega_{jr} T_i \right], \quad r = 1, \ldots, 4 \tag{36}$$

and the four dynamical equations of motion of the system can now be stated as

$$F_r + F_r^* = 0, \quad r = 1, \ldots, 4 \tag{37}$$

These equations, together with equation (2), the constraint equation, govern all motions of the system. To bring them into a form suitable for solution with a digital computer, one may proceed as follows: differentiate equation (2) twice with respect to time and use equations (4), (6), (8), (11), (14), (16), (19), (20), (24)–(29), (32), (35) and (36) to express the resulting equation and equations (37) in the form

$$\sum_{j=1}^{5} P_{ij} \ddot{\theta}_j = Q_i, \quad i = 1, \ldots, 5 \tag{38}$$

where P_{ij} is a function of $\theta_1, \ldots, \theta_5$, whereas Q_i is a function of $\theta_1, \ldots, \theta_5, \dot{\theta}_1, \ldots, \dot{\theta}_5$. Next, solve equations (38) for $\ddot{\theta}_1, \ldots, \ddot{\theta}_5$, obtaining

$$\ddot{\theta}_i = R_i, \quad i = 1, \ldots, 5 \tag{39}$$

where R_i is a function of $\theta_1, \ldots, \theta_5, \dot{\theta}_1, \ldots, \dot{\theta}_5$. Finally, introduce ten new dependent variables $q_1, \ldots, q_{10}$ by taking

$$q_1 = \theta_1, \ldots, q_5 = \theta_5 \tag{40}$$

and

$$q_6 = \dot{\theta}_1, \ldots, q_{10} = \dot{\theta}_5 \tag{41}$$

Substitution from equations (40) into equations (41) then yields

$$\dot{q}_i = q_{i+5}, \quad i = 1, \ldots, 5 \tag{42}$$

and equations (41) combined with equations (39) give

$$\dot{q}_{i+5} = R_i, \quad i = 1, \ldots, 5 \tag{43}$$

where R_i may now be regarded as a function of $q_1, \ldots, q_{10}$.

To solve equations (42) and (43) numerically, it is necessary to assign initial values to $q_1, \ldots, q_{10}$. However, not all of these may be chosen arbitrarily, because one of equations (38) was obtained by differentiating equation (2) twice with respect to time, which has the effect of raising the order of the system. To obtain a set of initial values of $q_1, \ldots, q_{10}$

compatible with equation (2), one may assign arbitrary values to $q_1, \ldots, q_4$ and $q_6, \ldots, q_9$; solve equation (2) for q_5; and, after replacing θ's and $\dot{\theta}$'s in accordance with equations (40) and (41), use equation (5) to determine the initial value of q_{10}. The only part of this process that poses any problem is that of solving the nonlinear equation (2) for q_5, but this can be accomplished by using a recently devised procedure[2] which, applied to the case at hand, involves the following steps. After picking initial values for $q_1, \ldots, q_4$, let C be the constant

$$C = (Ls_2 c_3 + s_4)^2 + (-B + Ls_2 s_3 + c_4)^2 + L^2 c_2^2 - (l'/l) L^2$$

where s_i and c_i now denote $\sin q_i$ and $\cos q_i$, respectively. Regard q_5 as a function of a dimensionless variable ξ, and solve the differential equation

$$\frac{dq_5}{d\xi} = \frac{1}{2} \frac{C}{\beta_5} \tag{44}$$

(see equations (4) for β_5) in the interval $0 \leqslant \xi \leqslant 1$, taking q_5 equal to zero at $\xi = 0$. Then the value obtained for q_5 at $\xi = 1$ is a solution of equation (2) corresponding to the chosen values of $q_1, \ldots, q_4$.

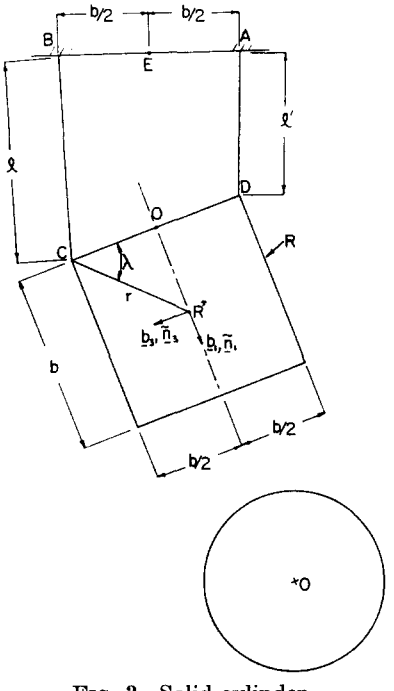

FIG. 3. Solid cylinder.

A study of the behavior of a body suspended from two cables of unequal length provides a practical application for the equations derived above, for the extent to which cable length inequality downgrades the performance of the bifilar pendulum can be assessed by reference to plots constructed with the aid of these equations. Suppose, for example, that the suspended body is a solid right-circular cylinder whose height and diameter are equal to the distance b between the points of attachment of the cables to the overhead support (see Fig. 1), and let the cables be attached to the cylinder at opposite ends of a diameter of one base (see Fig. 3). Then, if the cable lengths are $l = 2b$ and $l' = 1{\cdot}8b$, the remaining constants required for substitution into the equations of motion have the

values

$$r = b/\sqrt{2}, \qquad \lambda = \pi/4$$

$$I_1 = mb^2/8, \quad I_2 = I_3 = 7mb^2/48$$

$$[\tilde{b}_{ij}] = \begin{bmatrix} 1 & 0 & 0 \\ 0 & 1 & 0 \\ 0 & 0 & 1 \end{bmatrix}$$

and a physically meaningful set of initial conditions is obtained by imagining that the system is released from rest in a position in which $\theta_1, \ldots, \theta_4$ (see Fig. 1) have the values that they would have if $l' = l$ and the cylinder were raised vertically by rotating it through an angle of 45° about its axis of symmetry, with the cables taut. This state is described by [see equations (40) and (41)]

$$q_1 = 0, \quad q_2 = \arcsin[\tfrac{1}{2}\sin(\pi/8)], \quad q_3 = 7\pi/8, \quad q_4 = \pi/4 \quad q_6 = q_7 = q_8 = q_9 = 0$$

and the ensuing motion is characterized by the plots shown in Figs. 4, 5 and 6, these representing results of a numerical integration of the equations of motion. In each of

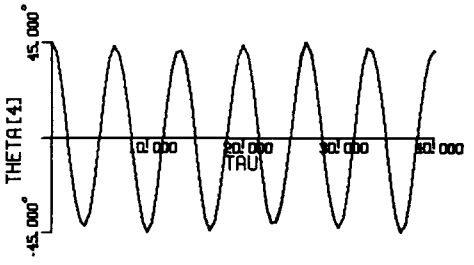

FIG. 4. Torsion; $l = 2b$, $l' = 1{\cdot}8b$.

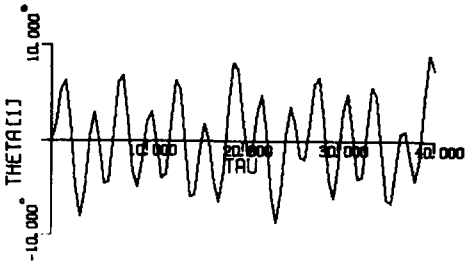

FIG. 5. Tilting; $l = 2b$, $l' = 1{\cdot}8b$.

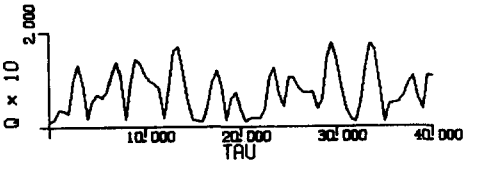

FIG. 6. Side-sway; $l = 2b$, $l' = 1{\cdot}8b$.

these plots, the abscissa measures a quantity τ that is proportional to time t, namely $\tau = (g/b')^{\frac{1}{2}} t$. Fig. 4 deals with "torsion", Fig. 5 furnishes a measure of "tilting" and the quantity Q plotted in Fig. 6 is the ratio to b' of the orthogonal projection of EO (see Fig. 3) on a horizontal plane. Hence this plot describes what may be termed "side-sway".

It appears from Fig. 4 that torsional oscillations proceed in a regular manner, despite the fact that one cable is 10 per cent shorter than the other. The cable length inequality

makes itself felt, however, by giving rise to the tilting oscillations depicted in Fig. 5 and by causing a considerable amount of side-sway, as indicated in Fig. 6. As might be expected, the amplitudes of these oscillations can be reduced by making the cable lengths more nearly equal. For instance, when the difference in lengths is decreased to one-fourth of its former value, i.e. l' is changed from $1{\cdot}8b$ to $1{\cdot}95b$, the maximum values of θ_1 and Q are reduced by about the same factor, as may be seen in Figs. 7 and 8. In the case of

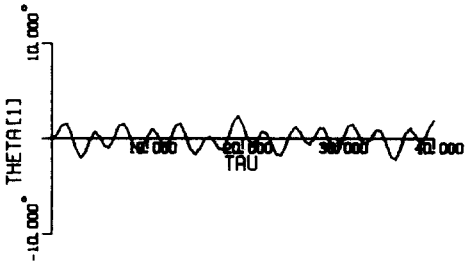

FIG. 7. Tilting; $l = 2b$, $l' = 1{\cdot}95b$.

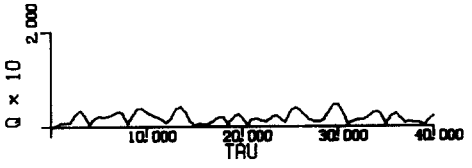

FIG. 8. Side-sway; $l = 2b$, $l' = 1{\cdot}95b$.

θ_1, the reduction in amplitude is accompanied by a considerable decrease in frequency, which means that the tilting oscillations have a fundamentally nonlinear character. This observation is of interest in connexion with stability questions, as will be seen later.

When the bifilar pendulum is used for moment of inertia determinations, the cables are usually attached in such a way that both are vertical and parallel to a principal axis for the mass center of the suspended body when the system is at rest. Torsional oscillations can then occur without accompanying tilting or side-sway. To find out whether or not misalignment of principal axes modifies the motion significantly, we consider an example involving pronounced misalignment, namely that of a thin triangular plate suspended as shown in Fig. 9.

The principal axes of the plate for the mass center R* are the lines R*D, R*C and a line passing through R* and normal to the plane of the plate. The associated moments of inertia have the values

$$I_1 = mb^2/16, \quad I_2\, 3mb^2/16, \quad I_3 = mb^2/14$$

while

$$[\check{b}_{ij}] = \frac{1}{\sqrt{2}} \begin{bmatrix} -1 & 0 & -1 \\ -1 & 0 & 1 \\ 0 & \sqrt{2} & 0 \end{bmatrix}$$

and, as in the previous example,

$$r = b/\sqrt{2}, \quad \lambda = \pi/4$$

If the plate is released from rest after being rotated through an angle of 45° about the line passing through O and E (see Fig. 9), the initial conditions are the same as in the preceding example and the subsequent motion proceeds in such a way that θ_4, θ_1 and Q vary with τ as shown in Figs. 10, 11 and 12. These plots reveal, perhaps surprisingly, that even rather severe misalignment of principal axes need not disturb the torsional motion very much (Fig. 10) and may lead to tilting (Fig. 11) and side-sway (Fig. 12) no

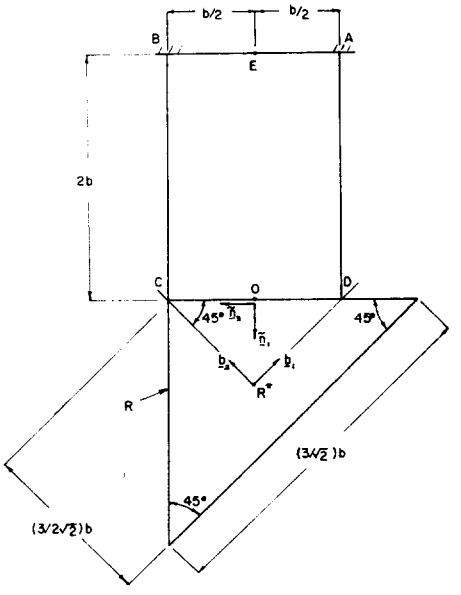

FIG. 9. Triangular plate.

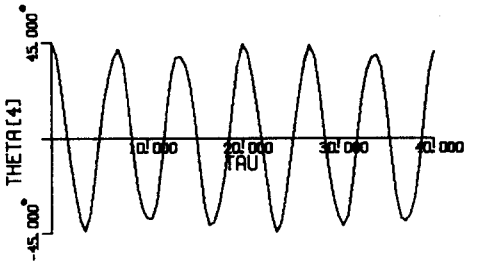

FIG. 10. Torsion.

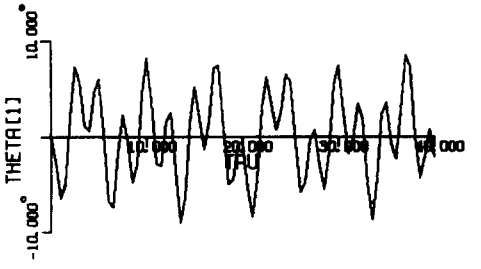

FIG. 11. Tilting.

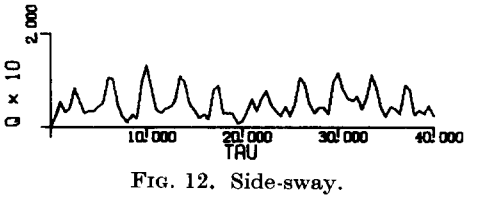

FIG. 12. Side-sway.

more violent than those attributable to a 10 per cent difference in cable lengths, as in the previous example (Figs. 5 and 6). In situations of the kind under consideration, a theory in which titling and side-sway are left out of account may, therefore, be expected to yield satisfactory results.

STABILITY OF TORSIONAL OSCILLATIONS

In practical applications of the bifilar pendulum one sometimes encounters the following phenomenon: soon after apparently purely torsional oscillations have been initiated, tilting oscillations are observed, and these become more pronounced with each successive swing. A change in the geometry of the suspension, e.g. in cable lengths or distances between points of attachment, can then have a stabilizing effect, i.e. subsequent to the change, torsional oscillations proceed without noticeable tilting. It is the purpose of what follows to establish a mathematical basis for predicting such events.

Confining attention to situations in which the cables are of equal length and the inertia properties of the suspended body are such that, when the body is at rest, its mass center lies on the vertical bisector of line AB (see Fig. 1) and one principal axis for the mass center is vertical, one may expect on grounds of "symmetry", and it can be verified by reference to the equations of motion, equations (37), that the following is a possible motion: purely vertical oscillations of the mass center are accompanied by torsional oscillations of the body about the vertical line passing through the mass center. It follows from equations (42) and (43) that, during such motion, q_4 and q_9 [see equations (40) and (41)] are governed by the pair of differential equations [see equations (42) and (43)]

$$\dot{q}_4 = q_9 \tag{45}$$

$$\dot{q}_9 = N_1(N_2 q_9^2 + N_3) \tag{46}$$

where N_1, N_2 and N_3 are functions of q_4, and the remaining q's either vanish or depend only on q_4 and q_9. Specifically,

$$\left.\begin{aligned} N_1 &= -[I_1 + mf(b^2/4l)^2 \sin^2 q_4]^{-1} \\ N_2 &= mf(b^2/4l)^2 [\cos q_4 + f(b/2l)^2 \sin^2 q_4] \sin q_4 \\ N_3 &= mg\sqrt{(f)}\,(b^2/4l) \sin q_4 \end{aligned}\right\} \tag{47}$$

where

$$f = \{1 - [(b/l) \sin (q_4/2)]^2\}^{-1} \tag{48}$$

and the q's are given by

$$\left.\begin{aligned} q_1 &= 0 & q_2 &= \arcsin [(b'/l) \sin (q_4/2)] \\ q_3 &= \pi - q_4/2 & q_5 &= 0 \\ q_6 &= 0 & q_7 &= (b/2l)\sqrt{(f)}\, q_9 \cos (q_4/2) \\ q_8 &= -q_9/2 & q_{10} &= 0 \end{aligned}\right\} \tag{49}$$

Substitution from equation (45) into equation (46) leads to a second-order differential equation in q_4. This equation possesses an oscillatory solution whose period t^* depends on the amplitude of the oscillations, and t^* can be found by a numerical integration of equations (45) and (46). Division of equation (46) by equation (45) has the effect of eliminating the time t, and it follows that q_9 is a function of q_4 only. Thus it appears that, during the motion under consideration, $q_1, \ldots, q_{10}$ all are periodic functions of the same period t^*. These functions will henceforth be denoted by $q_1^*, \ldots, q_{10}^*$, and they can always be generated explicitly by a numerical solution of equations (45) and (46) together with equations (47)–(49).

A description of any motion that differs from the one just considered is obtained by taking

$$q_i = q_i^* + \varepsilon_i, \quad i = 1, \ldots, 10 \tag{50}$$

where ε_i is a function of t. When these expressions are substituted into equations (42) and (43), and all terms of second or higher degree in the ε's and/or their time-derivatives

are dropped, the resulting equations assume the form

$$\dot{\varepsilon}_i = \sum_{j=1}^{10} Z_{ij}\,\varepsilon_j, \quad i = 1, \ldots, 10 \tag{51}$$

where Z_{ij} is a known function of $q_1^*, \ldots, q_{10}^*$ and may, therefore, be regarded as a periodic function of t, of period t^*. The behavior of the solutions of equations (51) characterizes the stability of the solution $q_i = q_i^*$, $i = 1, \ldots, 10$, of equations (42) and (43), in the following sense: when $\varepsilon_1(t), \ldots, \varepsilon_{10}(t)$ cannot be kept arbitrarily small for $t > 0$ by assigning sufficiently small values to $\varepsilon_1(0), \ldots, \varepsilon_{10}(0)$, then one or more of $|\, q_i(t) - q_i^*(t)\,|$, $i = 1, \ldots, 10$, cannot be kept arbitrarily small for $t > 0$ by assigning sufficiently small values to $|\, q_i(0) - q_i^*(0)\,|$, $i = 1, \ldots, 10$. The motion described by $q_i = q_i^*$, $i = 1, \ldots, 10$, is then said to be unstable. Now, the necessary information about the behavior of the solutions of equations (51) is furnished by Floquet theory.[3] The application of this theory to the problem at hand involves the following steps: letting $H(t)$ be a 10×10 matrix whose elements are functions of time t, and taking $H(0) = I$, the 10×10 unit matrix, integrate the differential equation

$$\frac{dH}{dt} = ZH$$

where Z is the 10×10 matrix having Z_{ij} as the element in the ith row and jth column. Terminate the integration at $t = t^*$, and find the eigenvalues $\lambda_1, \ldots, \lambda_{10}$ of the matrix $H(t^*)$. If the modulus of any one of these exceeds unity, then equations (51) possess solutions that cannot be kept arbitrarily small by assigning sufficiently small values to $\varepsilon_1(0), \ldots, \varepsilon_{10}(0)$. The associated motion $q_i = q_i^*$ is then unstable. The physical significance of one such instability is illustrated by the example that follows.

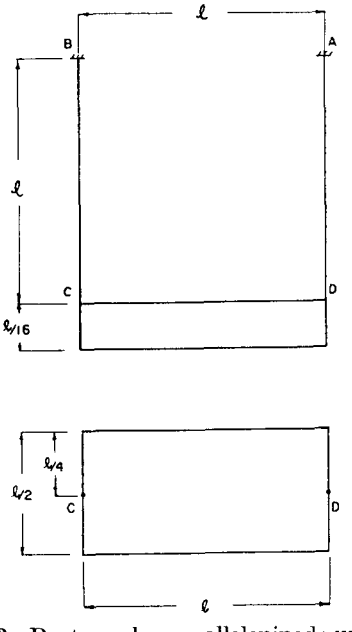

FIG. 13. Rectangular parallelepiped; unstable.

Fig. 13 shows a rectangular parallelepiped suspended from two equally long cables attached to the midpoints of two sides. When the procedure described above is applied to test the stability of torsional oscillations during which θ_4 has an amplitude of 45°, the modulus of one of the quantities $\lambda_1, \ldots, \lambda_{10}$ is found to have the value 2643, and the motion under consideration must thus be termed unstable. If one now integrates the full nonlinear equations of motion, equations (42) and (43), assigning to q_1 the small initial value

of 0·01 rad., and using for the remaining q's initial values appropriate to a pure torsional oscillation with an amplitude of 45°, one obtains the plot shown in Fig. 14, in which the previously mentioned tilting motion comes into evidence in rather dramatic fashion.

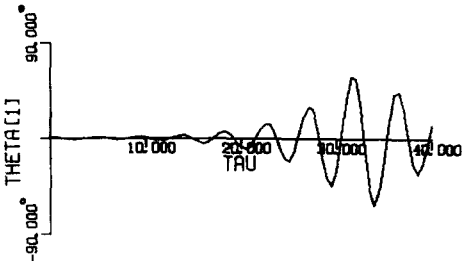

FIG. 14. Unstable tilting.

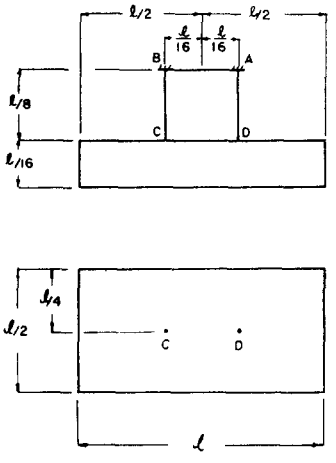

FIG. 15. Rectangular parallelepiped; stable.

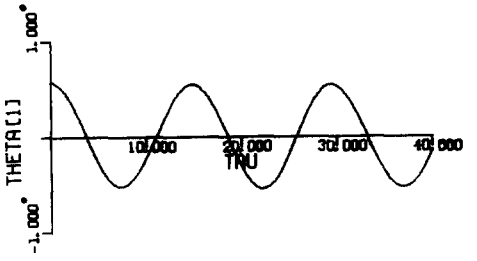

FIG. 16. Stable tilting.

In view of the instability just encountered, the arrangement shown in Fig. 13 must be regarded as unsuitable for an experimental determination of the moment of inertia I_1. To discover a satisfactory method of suspension, one can in such a case use the stability analysis for various combinations of b and l until one is found that does not lead to a prediction of instability. One such scheme is represented by Fig. 15. Initial conditions identical to those used to obtain Fig. 14 now lead to Fig. 16, and it is apparent that changing the method of suspension has brought about a fundamental change in the character of the tilting oscillations.

CONCLUSIONS

Inequality of cable lengths and pronounced misalignment of principal axes of inertia both have relatively little effect on torsional oscillations, but cause tilting and side-sway. Catastrophic tilting oscillations can occur even if the cables have equal lengths and the principal axes are perfectly aligned, but this instability can be eliminated by changing the geometry of the suspension.

REFERENCES

1. T. R. KANE, *J. appl. Mech.* **83**, 574 (1961).
2. T. R. KANE, *AIAA Jl*, to be published.
3. L. CESARI, *Asymptotic Behavior and Stability Problems in Ordinary Differential Equations*, pp. 55–58. Academic Press, New York (1963).